



Materials and Energy Research Center

MERC

Contents lists available at [ACERP](#)

Advanced Ceramics Progress

Journal Homepage: [www.acerp.ir](http://www.acerp.ir)

Advanced Ceramics Progress

## Original Research Article

# Fabrication and Evaluation of a Polydimethylsiloxane-Based Elastomeric Dental Impression Material with Ceramic Fillers

Mohsen Fakoori <sup>a</sup>, Saeed Hesaraki <sup>b\*</sup>, Nader Nezafati <sup>c</sup>, Majid Ghiass <sup>d</sup><sup>a</sup> PhD Student, Department of Nanotechnology and Advanced Materials, Materials and Energy Research Center, Karaj, Iran.<sup>b</sup> Professor, Department of Nanotechnology and Advanced Materials, Materials and Energy Research Center, Karaj, Iran.<sup>c</sup> Associate professor, Department of Nanotechnology and Advanced Materials, Materials and Energy Research Center, Karaj, Iran.<sup>d</sup> Assistant professor, Department of Novel Drug Delivery Systems, Iran Polymer and Petrochemical Institute (IPPI), Tehran, Iran.\* Corresponding Author Email: [s-hesaraki@merc.ac.ir](mailto:s-hesaraki@merc.ac.ir) (S.Hesaraki)URL: [https://www.acerp.ir/article\\_224892.html](https://www.acerp.ir/article_224892.html)

## ARTICLE INFO

## Article History:

Received: 25 May 2025

Revised: 14 June 2025

Accepted: 13 July 2025

## Keywords:

Condensation Silicone,  
Dental Impression Material,  
Dimensional Stability,  
Rheology,  
Polydimethylsiloxane

## ABSTRACT

Dental impression materials are fundamental to the production of accurate dental prostheses and restorations. This study focused on the formulation and characterization of a novel, plasticizer-free condensation silicone paste, comparing its performance to a commercial benchmark, Speedex. A specific laboratory paste was developed using 39 vol% hydroxy-terminated polydimethylsiloxanes (PDMS-OH), a high concentration of inorganic fillers (60 vol% silica and calcite), and 1 vol% tetraethyl orthosilicate (TEOS). In contrast, characterization of Speedex revealed a lower inorganic filler content of approximately 40 wt% and the likely presence of plasticizers. A detailed comparative analysis of physicochemical, rheological, and mechanical properties was conducted. The high-filler laboratory formulation demonstrated significantly improved dimensional stability, exhibiting less shrinkage over 12 hours compared to Speedex. This enhancement, however, resulted in a predictable trade-off in mechanical properties. The formulated paste was substantially stiffer, with a higher elastic modulus ( $4.8 \pm 0.2$  MPa vs.  $3.63 \pm 0.12$  MPa) and a slightly greater Shore A hardness (62 vs. 60), but it showed markedly reduced ductility, with a lower elongation at break (36.69% vs. 51.82%) than the more flexible commercial material. Rheological profiles also differed notably, reflecting their distinct compositions. These findings highlight that a high-filler, plasticizer-free formulation strategy can significantly improve dimensional accuracy, albeit at the cost of reduced flexibility, providing valuable insights into the structure-property relationships that govern the performance of condensation silicone impression materials.

<https://doi.org/10.30501/acp.2025.526078.1176>

## 1. INTRODUCTION

The accuracy and precision of dental impressions are paramount in ensuring the fabrication of well-fitting prostheses, orthodontic appliances, and dental restoration ([Giachetti et al., 2020](#)). These impressions form the foundation of a wide array of dental treatments, and their fidelity directly impacts the fit, function, and longevity of final restorations ([Pesce et al., 2024](#)). Historically, impression materials have

evolved from rigid substances such as plaster to elastic alternatives like agar and alginate, which had notable limitations in accuracy and detail capture ([Cervino et al., 2018](#)). The advent of elastomeric impression materials marked a significant advancement in dentistry, offering improved accuracy, dimensional stability, and the capacity to reproduce fine anatomical detail ([Haoran, 2022](#)). Among the various impression materials available, condensation silicones have been widely adopted in clinical practice ([Flügge et al., 2018](#)).

Please cite this article as: Fakoori, M. , Hesaraki, S. , Nezafati, N. & Ghiass, M. (2024). Fabrication And Evaluation of a Polydimethylsiloxane-Based Elastomeric Dental Impression Material with Ceramic Fillers, *Advanced Ceramics Progress*, 11(1), 7-18. <https://doi.org/10.30501/acp.2025.526078.1176>



This preference is due to their advantageous characteristics, including excellent dimensional stability, the ability to replicate intricate anatomical details, ease of handling, good elastic recovery, and cost-effectiveness ([Papaspolidakos et al., 2020](#)). Typically, these materials consist of a hydroxy-terminated polydimethylsiloxane (PDMS-OH) base polymer, inorganic fillers, a crosslinking agent such as tetraethyl orthosilicate (TEOS), and a catalyst to control the setting reaction and final properties ([Fakoori et al., 2025](#)).

Despite their widespread use, condensation silicones are not without limitations ([R. Mohd et al., 2021](#)). A primary concern is polymerization shrinkage, which occurs due to the release of volatile byproducts, commonly ethanol, during the condensation reaction ([Kundie et al., 2018](#)). This shrinkage can compromise dimensional accuracy and, consequently, the fit of dental prostheses ([Albanchez et al., 2020](#)). Achieving optimal rheological behavior and suitable mechanical properties remains a key challenge in their formulation ([Grundke et al., 2008](#)).

To address these limitations and enhance material properties, modifications to the formulation, particularly through the incorporation and selection of fillers, are common. Fillers are essential because the base PDMS-OH polymer alone is a liquid and lacks the necessary viscosity, body, and mechanical strength required for clinical application ([Abhijeet et al., 2022](#)). The type, size, concentration, and morphology of fillers play a crucial role and can significantly influence the physical, mechanical, and rheological properties of the final impression material ([REDDY et al., 2024](#)).

While modifications to silicone impression materials have been reported, detailed comparative analyses between commercial products and systematically formulated laboratory counterparts are relatively rare. A significant gap exists in understanding the direct performance trade-offs when a laboratory formulation is deliberately designed with a divergent strategy—in this case, high filler loading without plasticizers—to achieve handling characteristics similar to a plasticizer-containing commercial material. Therefore, the present study was undertaken to first comprehensively characterize the commercial condensation silicone, Speedex, to establish its baseline compositional strategy and property profile. Following this, a laboratory paste was formulated using a high-filler-content approach. The primary and novel objective of this research was to conduct a systematic, head-to-head comparison to elucidate the distinct property spectrums and inherent trade-offs (e.g., dimensional stability versus ductility) that arise directly from these opposing formulation philosophies. This work moves beyond simple material enhancement to offer a clear model of how fundamental

compositional choices dictate clinically relevant performance.

## 2. MATERIALS AND METHODS

### 2.1. Materials Used

The materials utilized in this research were as follows: Commercial condensation silicone impression paste Speedex Putty and its universal activator (Speedex Universal Activator; Coltène/Whaledent, Switzerland), procured from the Iranian dental market. For the preparation of the laboratory base paste, the following materials were used: Hydroxy-terminated polydimethylsiloxane (PDMS-OH) (viscosity: 5000 cP; Sigma-Aldrich, Germany); Silica powder (SiO<sub>2</sub>) (average particle size: 25 microns, density: 2.65 g/cm<sup>3</sup>; Neutron Shimi Co., Iran); Calcium carbonate powder (CaCO<sub>3</sub>) (density: 2.71 g/cm<sup>3</sup>; Merck, Germany); and Tetraethyl orthosilicate (TEOS) (density: 0.93 g/cm<sup>3</sup>; Merck, Germany) as a crosslinking agent. For solvent extraction tests, laboratory grade toluene and absolute ethanol (both from Merck, Germany) were used.

### 2.2. Preparation of Laboratory Base Paste

Following the initial characterization of the commercial Speedex material, which identified its primary polymeric and inorganic components (PDMS, quartz, calcite), a laboratory base paste was formulated using similar materials. The component ratios of hydroxy-terminated polydimethylsiloxane (PDMS-OH), silica powder, calcium carbonate powder, and tetraethyl orthosilicate (TEOS) were systematically adjusted. The formulation detailed below, (PDMS-OH (39 vol%), TEOS (1 vol%), silica (54 vol%), and calcium carbonate (6 vol%)), was selected for further study because its initial, simple visual and tactile handling characteristics were found to be comparable to those of the commercial Speedex paste upon preliminary assessment. This process resulted in a laboratory paste consisting of a liquid phase comprising hydroxy-terminated polydimethylsiloxane (PDMS-OH) (39 vol%) and tetraethyl orthosilicate (TEOS) (1 vol%) as the crosslinking agent. The inorganic filler phase (totaling 60 vol%) was a mixture of silica (SiO<sub>2</sub>) powder (54 vol%) and calcium carbonate (CaCO<sub>3</sub>) powder (6 vol%). Notably, this empirically selected formulation did not include plasticizers (which were suspected in the commercial material based on its characterization) and, due to the formulation strategy aimed at mimicking the initial handling properties, possessed a higher inorganic filler content (60 vol%) compared to the estimated inorganic content of Speedex (approx. 40 wt%). As schematically illustrated in Figure 1, the preparation involved weighing the fillers (silica and calcium carbonate) in the specified ratio, followed by thorough mixing and homogenization for 2 hours at a speed of 400 rpm using a planetary ball mill (model AS-2600; Bonyan Faragir Sanat Mehrebi Co.). The resulting

powder was then dried in an oven at 100°C for 24 hours. Thereafter, PDMS-OH and TEOS were gradually added to the filler mixture and mixed for one hour at an appropriate speed using a mechanical stirrer (IKA®RW 20 digital) until a homogeneous and uniform paste was obtained.

### 2.3. Preparation of Dies and Samples

To evaluate the linear dimensional stability of the commercial paste samples and the laboratory formulation, a standard ruler block (diameter: 29.97 mm; total block height: 31.0 mm) and its corresponding mold (a ring with an internal diameter of 30.00 mm and height of 6.0 mm) were fabricated from polymethyl methacrylate (PMMA) with a smooth, polished surface, in accordance with ANSI/ADA No. 19 and ISO 4823 standards (Figure 2). The pastes, once mixed with the respective activator according to the manufacturer's instructions for the commercial sample, and with Speedex Universal Activator for the laboratory sample in a similar ratio to the commercial sample, were placed into this die, and the ruler block was used for shaping and compressing the materials. For the evaluation of tensile properties, dumbbell-shaped specimens were created using a die machined from stainless steel, constructed to meet ASTM D412 Die C specifications, which include a gauge length of 33 mm and a width of 6 mm. During fabrication, the die was placed on a polished sheet of high-density polyethylene (HDPE), and the prepared material pastes were loaded into the die cavity. An additional HDPE sheet was then used as an upper platen to press the material, ensuring the formation of a flat specimen surface. For Shore A hardness tests, specimens were prepared with a minimum thickness of 6 mm on a flat, parallel surface.

## 2.4. Characterization Methods

### 2.4.1. Fourier Transform Infrared Spectroscopy (FTIR) Analysis

To identify the functional groups and chemical structure of the polymeric component in the commercial Speedex paste and the laboratory control paste, FTIR spectroscopy was performed using a PerkinElmer Spectrum Two (USA) device. Spectra were recorded over a wavenumber range of 400  $\text{cm}^{-1}$  to 4000  $\text{cm}^{-1}$ .

### 2.4.2. X-ray Diffraction (XRD) Analysis

XRD analysis was employed to identify the crystalline phases present in the inorganic fillers of both the commercial Speedex paste and the laboratory control paste. For the commercial paste, samples were prepared in three different ways: (1) Original paste (Putty (Paste)): A sample of the commercial paste was analyzed directly without any prior preparation. (2) Paste after heat treatment (Putty (Thermal)): To remove the polymeric phase, a sample of the commercial paste was placed in an electric furnace (Azar Furnaces F11L, Iran) at 450 °C for 2 hours. The remaining gray powder was collected after cooling and used for analysis. (3) Paste after solvent extraction (Putty (Solvent)): 20 g of the commercial paste was dissolved in 50 g of toluene. The resulting solution was centrifuged for 10 minutes at 9000 rpm using a centrifuge (Universal 320, Germany). The separated solid precipitate was dried in an oven at 75 °C for 5 hours to remove any residual solvent, and the resulting powder was then used for XRD analysis. The laboratory base paste was also analyzed directly by XRD. All XRD analyses were performed on powdered or paste samples using a Seifert 3003 PTS diffractometer (Germany) with a  $\text{CuK}\alpha$  radiation source ( $\lambda = 1.542 \text{ \AA}$ ) over a  $2\theta$  angular range of 10° to 65°.

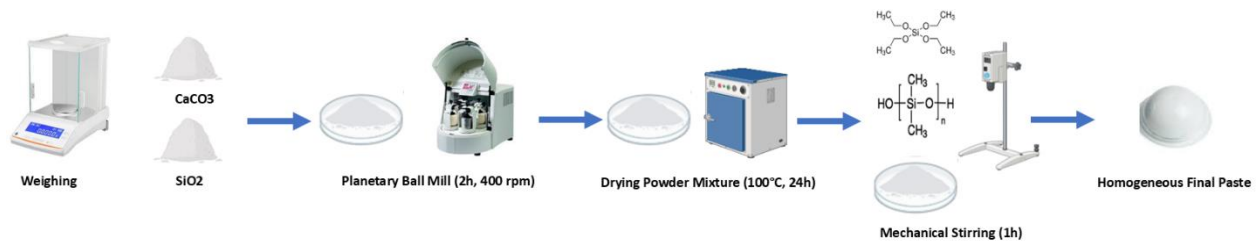


**Figure 1.** Schematic flowchart of the fabrication process for the laboratory base paste

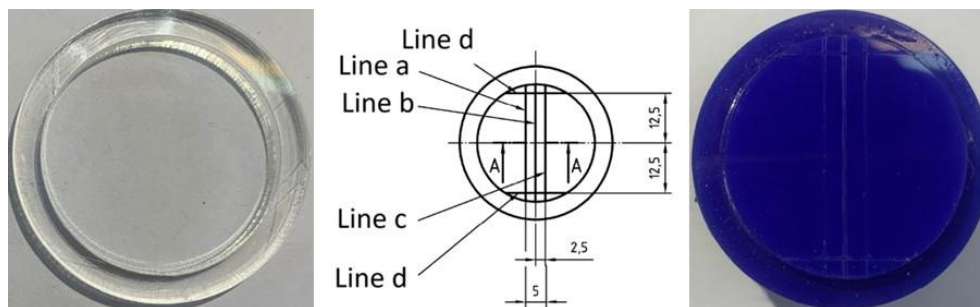


**Figure 2.** Fabricated ruler block for measuring linear dimensional changes (ISO 4823)

#### 2.4.3. Simultaneous Thermal Analysis (STA: TGA/DSC)

The thermal behavior and stability of the commercial Speedex paste were investigated using a simultaneous thermal analyzer (BAHR-STA-503, Germany). A sample of approximately 10–15 mg was placed in an alumina crucible and heated in an air atmosphere at a heating rate of 10 °C/min from ambient temperature (20 °C) up to 1000 °C. Weight change (TGA) and heat flow (DSC) curves were recorded simultaneously.

#### 2.4.4. Determination of Filler to Oil Ratio (for Commercial Paste)

The solvent extraction method was used to determine the weight ratio of filler to the polymeric component (oil) in the commercial Speedex Putty paste. A 10 g sample of the paste was accurately weighed and dissolved in 40 g of toluene. After complete dissolution of the polymeric part using a magnetic stirrer, the solution was centrifuged for 15 minutes at 9000 rpm to separate the solid and liquid phases. The upper liquid phase (containing the polymer dissolved in toluene) was carefully separated and transferred to a pre-weighed beaker. It was then stirred with a magnetic stirrer at 50 °C for 24 hours under a fume hood until only the polymeric oil remained. The solid filler retained in the centrifuge tube was dried in an oven at 75 °C for 72 hours. The weights of the dried filler and polymeric oil were measured, and the weight percentage of each component was calculated.

#### 2.4.5. Rheological Analysis

The rheological properties of the commercial Speedex paste and the laboratory base paste were examined using an Anton Paar Physica MCR 301 rotational rheometer at 25 °C. Experiments were conducted in both rotational mode to determine viscosity as a function of shear rate and oscillatory mode to evaluate storage modulus ( $G'$ ) and loss modulus ( $G''$ ).

#### 2.4.6. Mixing, Working, and Setting Times

The mixing, working, and setting times for the commercial Speedex paste and the laboratory-prepared paste were evaluated according to the ISO 4823 standard, with five repetitions for each test ( $n = 5$ ) at 25°C. Mixing time was measured with a chronometer, starting from the initial contact between the base paste and activator until a homogeneous texture, in terms of color, was achieved. Working time was recorded from the beginning of mixing until the material lost its fluidity and began to exhibit elastic properties. For setting time, a Gilmore needle (needle tip diameter: 2.12 mm; weight: 113.4 g) was used. The needle was dropped onto the surface of the paste placed in the ring mold every 15 seconds; the timer was stopped when the

needle no longer made an impression on the surface of the material.

#### 2.4.7. Energy Dispersive X-ray Spectroscopy (EDAX) Elemental Analysis

To examine the elemental composition of the commercial Speedex paste (24 hours after setting), a TESCAN VEGA3 device equipped with an EDAX detector was used. Samples were examined following appropriate preparation procedures, including the creation of a fresh fracture and gold coating. Elemental mapping was also performed to assess the distribution of elements.

#### 2.4.8. Dimensional Stability Test

The dimensional stability of the commercial Speedex paste and the laboratory control paste was evaluated using molds prepared from a standard ruler block (Figure 1). Five replicate molds were prepared for each material ( $n = 5$ ). The paste and activator were mixed at 25°C, poured into the ring mold, and shaped using the ruler block. After setting, the distances between the parallel lines were measured using an OLYMPUS DP72 optical microscope at 30 minutes and 12 hours post-setting.

#### 2.4.9. Tensile Properties Test

The tensile properties of the set commercial Speedex and laboratory-prepared pastes were evaluated 24 hours after mixing with the activator using a SANTAM STM-20 device with a 1-ton capacity. Five dumbbell-shaped specimens ( $n = 5$ ) for each material type were prepared in accordance with ASTM D412 (Die C) specifications. Each specimen was subjected to a preload of 1 Newton at a crosshead speed of 5 mm/min, followed by an increase in speed to 500 mm/min until rupture. From the resulting stress-strain curves, the maximum force (N), extension (mm), percentage elongation (%), and elastic modulus (MPa) were determined.

#### 2.4.10. Shore A Hardness Test

The Shore A hardness of the set commercial Speedex and laboratory-prepared pastes was measured 24 hours after mixing, in accordance with ASTM D-2240. A Shore A-type analog portable durometer (Model SHD, SANTAM, Iran) was used. Specimens with a minimum thickness of 6 mm and flat, parallel surfaces were prepared. For each material type, three specimens were tested, and five hardness readings were taken at different points on each specimen ( $n = 3, 5$  readings per specimen) at room temperature (25°C). The mean hardness value was then calculated.

### 3. RESULTS AND DISCUSSION

#### 3.1. Thermal Analysis and Filler Percentage Determination of Commercial Paste (STA: TGA/DSC and Solvent Extraction)

The simultaneous thermal analysis (STA) curves of the commercial Speedex silicone impression paste are

shown in Figure 3. Thermogravimetric Analysis (TGA) indicates a multi-stage thermal decomposition process for the organic components of the paste. A total weight loss of approximately 60 wt% was observed up to about 580°C. This loss is attributed to the thermal decomposition and volatilization of the organic constituents—namely, the polydimethylsiloxane (PDMS) polymer, crosslinking agent, and any other organic additives such as plasticizers that may be present (Wang et al., 2021).

Three main stages of weight loss were discernible: First stage (ambient to ~280°C): An initial weight loss of ~10 wt%, likely corresponding to the evaporation of absorbed moisture or other highly volatile components; Second stage (~280 to ~330°C): A further weight decrease from ~90 wt% to ~75 wt% of the initial mass, which can be attributed to the onset of decomposition of the main polymeric chains; Third stage (~330 to ~580°C): The most significant weight loss occurred in this range, with the sample mass dropping from ~75 wt% to approximately 40 wt%. This stage reflects the more complete thermal degradation of the PDMS polymeric structure. After heating to 600°C and beyond, the sample weight stabilized at approximately 40 wt% of its initial mass (Mandal et al., 2024).

This residual mass represents the inorganic, thermally stable filler content of the commercial Speedex paste. The TGA-derived inorganic content of ~40 wt% aligns with the results obtained from the solvent extraction method (Table 1), which also indicated a similar proportion of insoluble inorganic material.

Differential Scanning Calorimetry (DSC) (Figure 3) revealed corresponding thermal events: an initial endothermic peak (~115–140°C) associated with the evaporation of volatile components; a subsequent endothermic event (~270–330°C), likely related to phase transitions or the early stages of polymer degradation; and a smaller exothermic peak (~335–370°C), possibly due to side reactions, structural rearrangements, or the decomposition of minor organic additives. The most prominent event was a large exothermic peak centered around 530–540°C (spanning ~480–600°C), indicative of the major oxidative decomposition of the PDMS polymer and other organic components (Utrera-Barrios et al., 2025).

These STA results suggest that the commercial Speedex paste is thermally stable up to approximately 280°C, above which its organic components begin to decompose, leaving behind a residual inorganic filler content of about 40 wt%. The remaining 60 wt% comprises the organic phase of the material.

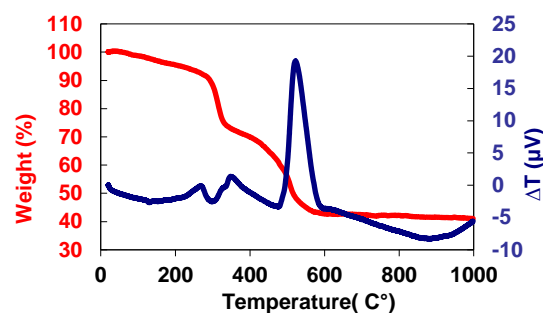


**Figure 3.** STA analysis (DSC and TGA curves) obtained from the commercial paste)

**TABLE 1.** Probable percentage of components in the commercial paste

| Material Type | Probable Amount Used |
|---------------|----------------------|
| Plasticizers  | 19 wt%               |
| TEOS          | 1 wt%                |
| PDMS          | 40 wt%               |
| Filler        | 40 wt%               |

## 3.2. Spectroscopic and Diffractometric (FTIR and XRD) Analyses

### 3.2.1. Commercial Speedex Paste: Chemical and Phase Characterization

#### 3.2.1.1. FTIR Analysis

The FTIR spectrum of the commercial Speedex (Putty) paste (Figure 4(a)) provided evidence for its chemical composition. The spectrum was dominated by characteristic absorption peaks of polydimethylsiloxane (PDMS), confirming it as the primary polymeric component. Key PDMS-related peaks included Si-CH<sub>3</sub> deformation vibrations (around 798 cm<sup>-1</sup> and ~1260 cm<sup>-1</sup>), the strong Si-O-Si stretching vibration (near 1014 cm<sup>-1</sup>), and a broad absorption band in the 3200-3700 cm<sup>-1</sup> region, attributed to Si-OH stretching from terminal hydroxyl groups on the PDMS-OH chains, indicative of hydrogen bonding. Other typical PDMS peaks, such as C-H stretching, were also observed. Notably, a peak around 1600 cm<sup>-1</sup> was present. This absorption is often associated with C=O stretching vibrations and, in the context of a silicone formulation with a significant organic content (as indicated by TGA), may suggest the presence of ester-based plasticizers or other carbonyl-containing additives.

#### 3.2.1.2. XRD Analysis

XRD patterns of the commercial Speedex paste, obtained from the original paste, heat-treated residue, and solvent-extracted residue (Figure 4(b)), were used to identify the crystalline inorganic phases. All three sample preparations consistently revealed quartz ( $\alpha$ -Quartz) and calcite (CaCO<sub>3</sub>) as the main crystalline fillers. Characteristic diffraction peaks for quartz were observed at 2 $\theta$  angles of approximately 21°, 26.7°, 36°, 50°, 60°, and 68°. Peaks corresponding to calcite were

identified at angles such as  $2\theta \approx 20.8^\circ$ ,  $29.4^\circ$ , and  $43.1^\circ$ . The similarity of the XRD patterns across the different sample states confirms the identity and stability of these filler components within the Speedex formulation.

### 3.2.2. Laboratory-Prepared Base Paste: Chemical and Phase Characterization

#### 3.2.2.1. FTIR Analysis

The FTIR spectrum of the laboratory-prepared base paste also clearly exhibited the characteristic absorption peaks of polydimethylsiloxane, consistent with its formulation. These included Si-CH<sub>3</sub> vibrations (around  $1261\text{ cm}^{-1}$  and  $797\text{ cm}^{-1}/857\text{ cm}^{-1}$ ), Si-O-Si stretching (around  $1024\text{ cm}^{-1}$  and  $1094\text{ cm}^{-1}$ ), C-H stretching ( $2905\text{ cm}^{-1}$ ,  $2965\text{ cm}^{-1}$ ), and a broad O-H stretching band around  $3700\text{ cm}^{-1}$  (from PDMS-OH and possibly absorbed moisture). Importantly, the distinct peak around  $1600\text{ cm}^{-1}$ , observed in the commercial Speedex spectrum and tentatively attributed to plasticizers, was absent in the laboratory paste's spectrum. This is consistent with the known formulation of the laboratory paste, which did not include plasticizers.

#### 3.2.2.2. XRD Analysis

The XRD pattern of the laboratory base paste (Figure 4(d)) was analyzed to confirm the crystalline nature of its inorganic fillers. The data verified the presence of quartz and calcite, which were the types of silica and calcium carbonate powders intentionally used in the laboratory formulation. Prominent quartz peaks

(at  $2\theta \approx 26.6^\circ$ ) and calcite peaks (at  $2\theta \approx 29.4^\circ$ ) were clearly visible.

### 3.3. Energy Dispersive X-ray Spectroscopy (EDX) and Elemental Mapping Analysis

SEM analysis of the commercial Speedex paste (Figure 5(a)) revealed a heterogeneous microstructure. Elemental mapping and EDX spectrum (Figure 5(b)) confirmed a widespread and uniform distribution of silicon (Si) and oxygen (O), consistent with the PDMS polymer and siliceous/carbonate fillers. Distinct, concentrated regions of Calcium (Ca), often overlapping with carbon (C) and oxygen (O), were indicative of CaCO<sub>3</sub> filler particles. Carbon (C) was widely distributed, attributable to both the polymer chain and carbonate fillers. The EDX spectrum presented in Figure 5(b) further confirms the presence of these elements. The characteristic silicon peak (SiK $\alpha$ ) displayed the highest intensity, reflecting its abundance in the sample composition. Significant intensity was also observed for the oxygen (OK $\alpha$ ) and calcium (CaK $\alpha$ ) peaks. The carbon peak (CK $\alpha$ ) was also clearly visible. Moreover, a smaller but distinct peak for magnesium (MgK $\alpha$ ) and a very weak signal for nitrogen (NK $\alpha$ ) were recorded. These spectral data are consistent with the elemental mapping results, confirming the heterogeneous elemental composition of the sample, which is predominated by silicon and calcium compounds, along with smaller amounts of magnesium compounds (Fakoori et al., 2025).

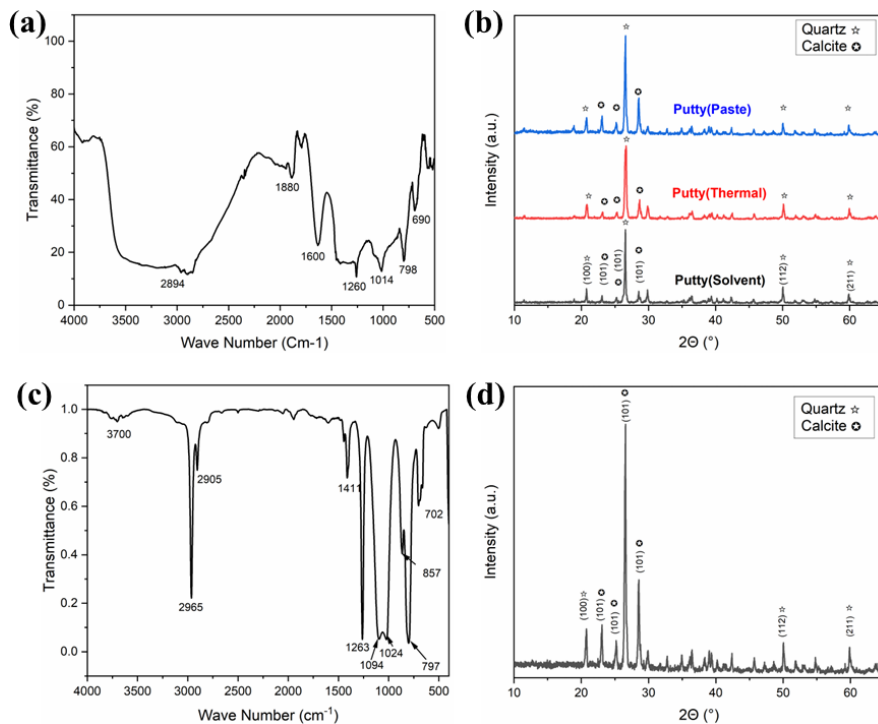


**Figure 4.** Spectroscopic and diffractometric analysis of the commercial and laboratory pastes: (a) FTIR spectrum of the commercial paste; (b) XRD patterns of the commercial paste (original, heat-treated, and solvent-extracted); (c) FTIR spectrum of the laboratory paste; and (d) XRD pattern of the laboratory paste.

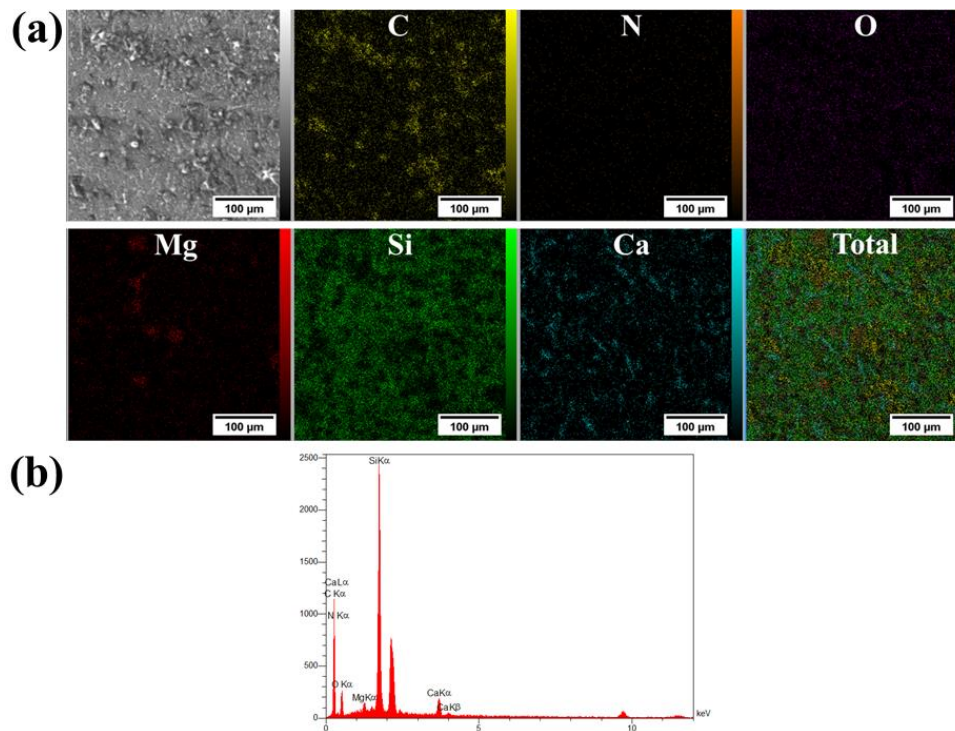


**Figure 5.** Microstructure and elemental composition of the commercial paste by: (a) SEM images and EDX mapping, (b) EDX spectrum

### 3.4. Characterization and Evaluation of Laboratory-Prepared Paste vs. Commercial Paste

#### 3.4.1. Rheological Analysis

The rheological properties of the two pastes were investigated to understand how their distinct formulations affect clinical handling and performance, which are critical for impression accuracy (Ibraheem, 2022) (Figure 6).

Both materials exhibited strong shear-thinning (pseudoplastic) behavior, which is advantageous for clinical application.

The analysis revealed that the custom paste displayed a significantly higher initial viscosity of approximately 10,000 Pa·s, more than double that of the commercial paste (~4,000 Pa·s), indicating that the custom formulation is substantially thicker and more resistant to slump at rest. While the torque required to initiate flow was higher for the commercial paste, its complex profile suggested a thixotropic nature not observed in the more conventional shear-thinning behavior of the custom material.

In oscillatory tests, the Commercial paste consistently showed a more robust viscoelastic character, with a higher storage modulus ( $G'$ ) of approximately 7,000 Pa compared to the Custom paste's ~5,000 Pa at 1 rad/s (Figure 6c). This indicates the commercial formulation has a more elastically resilient network, a finding supported by its higher loss modulus ( $G''$ ) and complex viscosity ( $\eta^*$ ) values as well.

The combined rheological data provide a clear rationale for the performance differences rooted in the two distinct formulation strategies. The custom paste's rheological profile, characterized by high viscosity at rest and pronounced shear-thinning, is consistent with its high-filler, plasticizer-free design. This type of shear-sensitive network is highly effective at providing body and resisting slump under low stress, a key factor that directly contributes to the material's superior dimensional stability, which was the primary performance benefit identified in this study. In contrast, the commercial paste's profile, with its higher elastic modulus and complex thixotropic behavior, reflects a formulation optimized for viscoelastic recovery and flexibility, likely enhanced by plasticizers. Therefore, the rheological behavior of each paste directly explains the specific trade-offs between dimensional accuracy and mechanical flexibility that were the focus of this investigation.

#### 3.4.2. Mixing, Working, and Setting Time Tests

The mixing, working, and setting times for the commercial Speedex paste and the laboratory paste were evaluated according to the ISO 4823 standard (Figure 7) (REDDY et al., 2024). Mixing Time (Figure 7a): The average mixing time for the commercial sample was approximately  $21 \pm 0.5$  seconds, and for the laboratory sample, about  $22 \pm 1.3$  seconds. Working Time (Figure 7b): The average working time for the commercial sample was recorded as  $45.8 \pm 1.1$  seconds, and for the laboratory sample,  $45 \pm 3$  seconds. Setting

Time (Figure 7c): The average setting time for the commercial sample was  $186 \pm 8$  seconds, and for the laboratory sample,  $190 \pm 6$  seconds. The results indicate that there were no statistically significant differences in mixing, working, or setting times between the commercial Speedex and the laboratory-prepared paste when using the same universal activator. This suggests

that the fundamental condensation polymerization kinetics are comparable for both materials under the specified test conditions, despite their distinct overall compositions (Hafezeqoran et al., 2021). While the defined timings are similar, the subjective handling feel during mixing and placement might still differ due to the rheological variations previously noted.

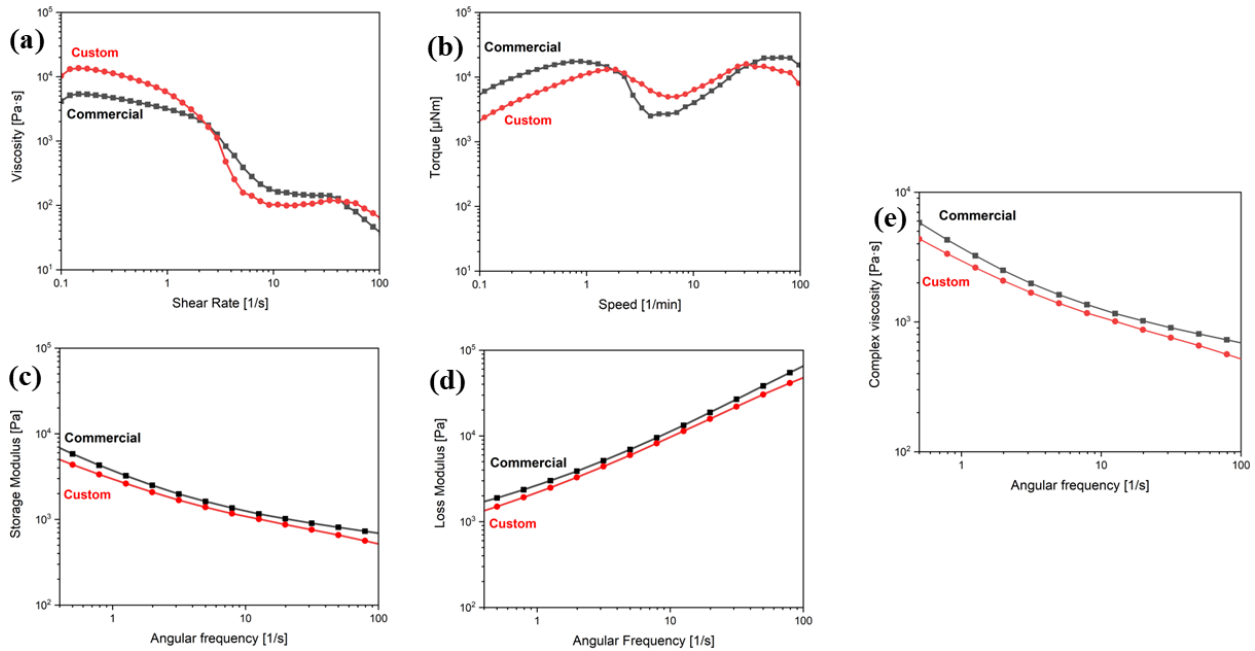


**Figure 6.** Comparative rheological graphs of commercial (Commercial/Speedex) and laboratory (Custom) silicone impression pastes. (a) Viscosity vs. Shear Rate, (b) Torque vs. Speed, (c) Storage Modulus ( $G'$ ) vs. Angular Frequency, (d) Loss Modulus ( $G''$ ) vs. Angular Frequency, and (e) Complex Viscosity ( $\eta^*$ ) vs. Angular Frequency.

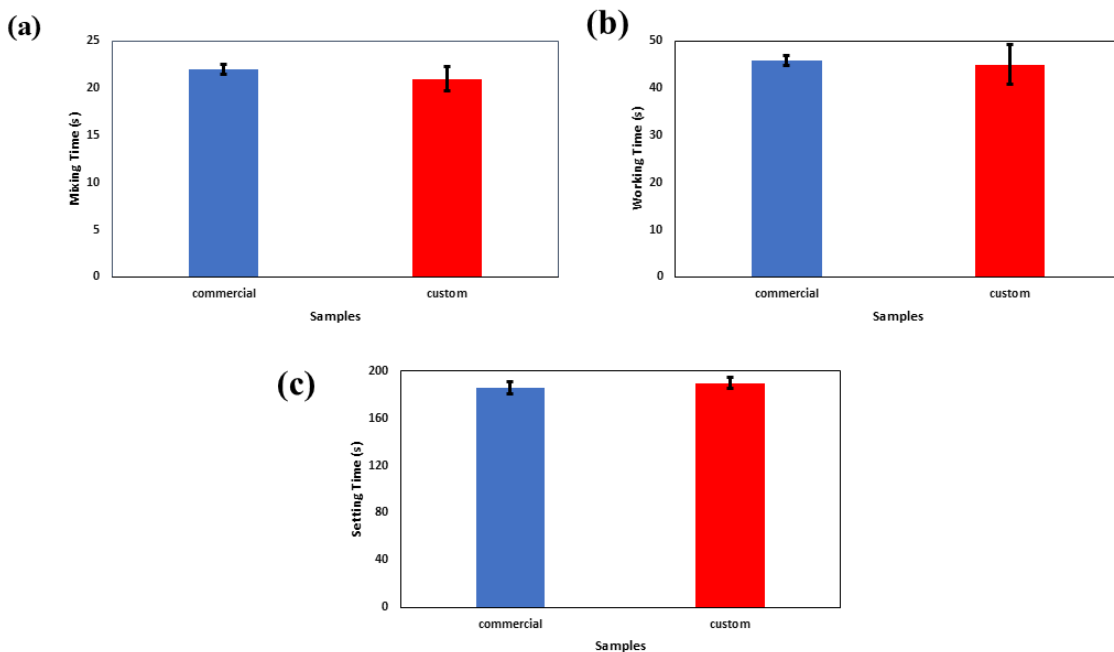


**Figure 7.** Comparison of (a) mixing time, (b) working time, and (c) setting time (seconds) of commercial and laboratory (Custom) silicone impression pastes. (Data are presented as mean  $\pm$  standard deviation for n=5 repetitions)

### 3.4.3. Dimensional Stability Test

Dimensional stability is a critical property for dental impression materials. In this study, it was evaluated using a standard ruler block according to ISO 4823, at both 30 minutes and 12 hours after setting (Figure 8). Both the commercial Speedex and the laboratory-prepared samples exhibited a decrease in linear dimensions (shrinkage) over time, which is an inherent characteristic of condensation silicones due to the release of volatile byproducts. However, a key finding from the statistical analysis was that the laboratory-prepared paste consistently demonstrated significantly less shrinkage than the commercial Speedex sample across all four measurement sets at both 30-minute and 12-hour time intervals ( $p < 0.05$  or  $p < 0.01$ ). This difference was especially pronounced at the 12-hour mark. For instance, as indicated by the statistical markers in Figure 8, the superior dimensional stability of the laboratory formulation is statistically significant in all comparisons. This enhanced dimensional stability of the laboratory paste can be attributed to its specific composition (Garg & Garg, 2021). The high volume of inert filler particles (60 vol%) in the custom paste physically limits volumetric shrinkage of the polymer matrix by reducing the relative amount of polymer undergoing condensation and subsequent byproduct evaporation. In contrast, the commercial Speedex contains a lower inorganic content and higher organic content, making it more susceptible to shrinkage. The superior dimensional stability of the laboratory-formulated paste is a significant performance advantage, essential for achieving accurate dental restorations (Alkurt et al., 2016).

### 3.4.4. Tensile Properties

The tensile properties of the set materials provide insights into their strength, flexibility, and toughness (Figure 9, Table 2).

**Maximum Force/Tensile Stress:** The commercial Speedex sample exhibited a marginally higher maximum force at break ( $29.92 \pm 0.98$  N) than the laboratory-prepared sample ( $27.96 \pm 1.01$  N), resulting in a marginally higher maximum tensile stress for Speedex. This suggests that the commercial formulation, likely benefiting from its higher polymer content and the toughening effect of plasticizers, offers slightly greater resistance to ultimate fracture.

**Elastic Modulus (Stiffness):** A notable difference was observed in the elastic modulus. The laboratory-prepared paste demonstrated a significantly higher elastic modulus ( $4.8 \pm 0.2$  MPa) compared to the commercial Speedex ( $3.63 \pm 0.12$  MPa), indicating it is substantially stiffer. This increased rigidity is directly attributed to its high inorganic filler content, which enhances reinforcement of the polymer matrix. The steeper initial slope of its stress-strain curve (Figure 9) visually confirms this greater stiffness.

**Extension and Elongation (%):** Conversely, the commercial Speedex sample showed markedly greater extension at break ( $17.10 \pm 0.4$  mm) and percentage elongation ( $51.82 \pm 1.14$  %) than the laboratory sample ( $12.10 \pm 0.21$  mm extension,  $36.69 \pm 1.26$  % elongation). This suggests that Speedex is considerably more ductile and flexible, capable of undergoing greater deformation before fracturing (Hassan et al., 2022). This flexibility is advantageous for removing impressions from undercut areas without tearing and is likely due to its lower filler content and the presence of plasticizers, which increase polymer chain mobility. The tensile property data reveal a classic trade-off. The laboratory-formulated paste, with its high filler content, achieves greater stiffness (elastic modulus), which can help resist deformation during model pouring and may enhance impression accuracy by preserving form. This complements its superior dimensional stability. However, this increased stiffness comes at the cost of reduced ductility (lower elongation at break), making the laboratory paste more brittle. In contrast, the commercial Speedex, though less stiff, offers significantly better flexibility—crucial for clinical usability in cases involving undercuts. These differences highlight how distinct formulation strategies (high conventional filler vs. moderate filler with plasticizers) produce markedly different mechanical profiles (Garg & Garg, 2021). The distinct mechanical profiles of the two materials carry direct clinical implications. The laboratory-formulated paste, with its high stiffness and superior dimensional stability, is ideally suited for high-precision applications where resistance to distortion is critical and dental undercuts are minimal. This includes impressions for single-unit crowns, bridges, and particularly implant-supported prostheses, where even slight micro-movements can compromise the final fit. However, its increased brittleness—resulting from its low ductility—poses a clinical risk. When used in areas with deep undercuts, the material may fracture during removal from the mouth. Conversely, the commercial Speedex formulation, with its notably greater flexibility and elongation, is the preferable option for impressions involving multiple teeth and pronounced undercuts, such as those required for removable partial dentures. Its flexibility facilitates safe removal without tearing, though clinicians must be mindful of its lower dimensional stability and ensure the cast is poured promptly to maintain accuracy.

### 3.4.5. Shore A hardness

Shore A hardness measures a material's resistance to indentation (TABLE 3). The laboratory-prepared paste exhibited a mean Shore A hardness of  $62 \pm 1.32$ , which was slightly higher than that of the commercial Speedex material, which recorded a value of  $60 \pm 1.16$ . This modestly higher hardness is consistent with the laboratory sample's greater elastic modulus and

inorganic filler content. Materials with a higher proportion of rigid filler particles and a stiffer matrix generally offer better resistance to localized surface deformation (Çevik, 2018). This property, along with stiffness, is important for maintaining the fine detail of the impression during gypsum pouring and subsequent

handling. When considered alongside its high stiffness and excellent dimensional stability, the laboratory paste's slightly superior hardness contributes to its overall profile as a material capable of producing rigid, dimensionally accurate impressions (Savin et al., 2019).

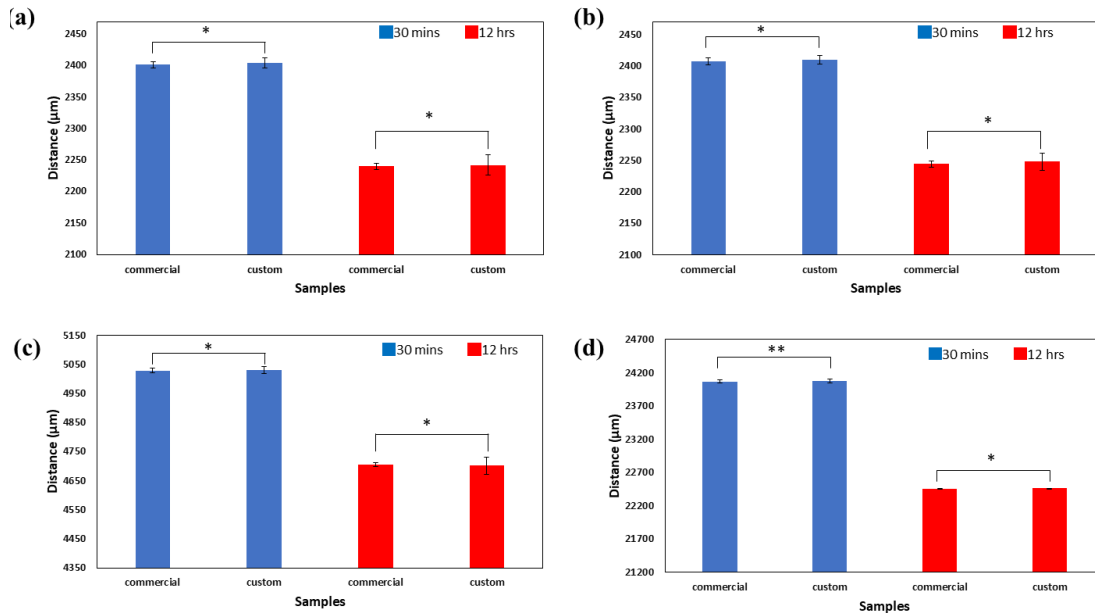


**Figure 8.** Comparison of linear dimensional changes (µm) of commercial and laboratory (Custom) silicone impression paste samples in four different measurement sets (a-d) at 30 minutes and 12 hours post-setting. Data are presented as mean ± standard deviation (n=5). Asterisks denote a statistically significant difference in dimensional change compared to the commercial sample at the same time point (\*p < 0.05, \*\* p < 0.01)

**TABLE 2.** Tensile properties of commercial (Speedex) and custom (laboratory-prepared) condensation silicone impression materials. Values are presented as mean ± standard deviation.

| Sample     | Force (N)      | Extension (mm) | Elongation (%) | Elastic Modulus (MPa) |
|------------|----------------|----------------|----------------|-----------------------|
| Commercial | 29.92 +/- 0.98 | 17.10 +/- 0.4  | 51.82 +/- 1.14 | 3.63 +/- 0.12         |
| Custom     | 27.96 +/- 1.01 | 12.10 +/- 0.21 | 36.69 +/- 1.26 | 4.8 +/- 0.2           |

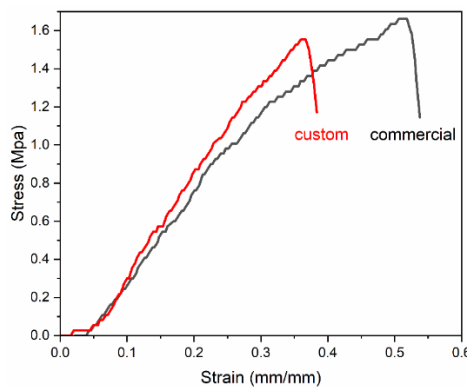


**Figure 9.** Representative stress-strain curves for the commercial and custom samples, illustrating their tensile behavior under uniaxial load.

**TABLE 3.** Shore A hardness values for commercial and custom samples. Values are presented as mean ± standard deviation.

| Samples    | Mean | Std. Deviation |
|------------|------|----------------|
| commercial | 60   | 1.16           |
| custom     | 62   | 1.32           |

#### 4. CONCLUSION

This study successfully demonstrated the distinct performance profiles resulting from two different formulation strategies for condensation silicone impression materials. By developing a plasticizer-free paste with a high inorganic filler content (60 vol%) and comparing it to a commercial benchmark (Speedex, containing ~40 wt% filler and suspected plasticizers), a critical trade-off was identified. The high-filler laboratory paste achieved markedly superior dimensional stability, a crucial property for clinical accuracy. However, this was achieved at the cost of increased stiffness and a significant reduction in ductility, rendering it more brittle than the flexible commercial material. This investigation underscores that the balance between the polymer-to-filler ratio and the inclusion of additives such as plasticizers directly governs the material's final properties. While the enhanced accuracy of the formulated paste is promising for precision applications such as implant prosthodontics, its brittleness must be considered in cases involving significant undercuts. Ultimately, this work provides a clear framework for how fundamental compositional choices can be used to tailor silicone impression materials to specific clinical needs, balancing the competing demands of dimensional accuracy and mechanical flexibility.

#### REFERENCES

- Abhijeet, K., Jei, J. B., Murugesan, K., & Muthukumar, B. (2022). Evaluation of setting time, tear strength, dimensional stability and antimicrobial property of silver and titanium nanoparticles incorporated elastomeric impression material. *Journal of Oral Biology and Craniofacial Research*, 12(5), 547–551. <https://doi.org/10.1016/j.jobcr.2022.07.002>
- Albanchez-Gonzalez, M. I., Brinkmann, J. C. B., Pelaez-Rico, J., Lopez-Suarez, C., Rodriguez-Alonso, V., & Suarez-Garcia, M. J. (2022). Accuracy of digital dental implants impression taking with intraoral scanners compared with conventional impression techniques: A systematic review of in vitro studies. *International journal of environmental research and public health*, 19(4), 2026. <https://doi.org/10.3390/ijerph19042026>
- Alkurt, M., Duymus, Z. Y., & Dedeoglu, N. (2016). Investigation of the effects of storage time on the dimensional accuracy of impression materials using cone beam computed tomography. *The Journal of Advanced Prosthodontics*, 8(5), 380–387. <https://doi.org/10.4047/jap.2016.8.5.380>
- Aslan, Y. U., & Özkan, Y. K. (2018). Impression Material Selection According to the Impression Technique. *Complete Denture Prosthodontics: Planning and Decision-Making*, 111–132. [https://doi.org/10.1007/978-3-319-69032-2\\_4](https://doi.org/10.1007/978-3-319-69032-2_4)
- Çevik, P. (2018). Evaluation of Shore A hardness of maxillofacial silicones: the effect of dark storage and nanoparticles. *European Oral Research*, 52(2), 99–104. <https://doi.org/10.26650/eor.2018.469>
- Cervino, G., Fiorillo, L., Herford, A. S., Laino, L., Troiano, G., Amoroso, G., ... & Ciccù, M. (2018). Alginate materials and dental impression technique: A current state of the art and application to dental practice. *Marine drugs*, 17(1), 18. <https://doi.org/10.3390/md17010018>
- Fakoori, M., Hesarak, S., Nezafati, N. et al. Evaluation of condensation silicone dental impression materials modified with diatomaceous Earth and zinc oxide fillers. *Sci Rep* 15, 25289 (2025). <https://doi.org/10.1038/s41598-025-11026-6>
- Flügge, T., van der Meer, W. J., Gonzalez, B. G., Vach, K., Wismeijer, D., & Wang, P. (2018). The accuracy of different dental impression techniques for implant-supported dental prostheses: A systematic review and meta-analysis. *Clinical oral implants research*, 29, 374–392. <https://doi.org/10.1111/clr.13273>
- Giachetti, L., Sarti, C., Cinelli, F., & Russo, D. S. (2020). Accuracy of digital impressions in fixed prosthodontics: a systematic review of clinical studies. *Int J Prosthodont*, 33(2), 192–201. [https://www.academia.edu/download/95431755/ijp\\_33\\_2\\_Giachetti\\_p192.pdf](https://www.academia.edu/download/95431755/ijp_33_2_Giachetti_p192.pdf)
- Grundke, K., Michel, S., Knispel, G., & Grundler, A. (2008). Wettability of silicone and polyether impression materials: Characterization by surface tension and contact angle measurements. *Colloids and Surfaces A: Physicochemical and Engineering Aspects*, 317(1–3), 598–609. <https://doi.org/10.1016/j.colsurfa.2007.11.046>
- Hafezeqoran, A., Rahbar, M., Koodaryan, R., & Molaei, T. (2021). Comparing the Dimensional Accuracy of Casts Obtained from Two Types of Silicone Impression Materials in Different Impression Techniques and Frequent Times of Cast Preparation. *International Journal of Dentistry*, 2021,9987453. <https://doi.org/10.1155/2021/9977478>
- Haoran, M. A. (2022). Digital Versus Conventional Impressions for Fixed Prosthodontics: A Review. *Jdoh*, 9(1), 1–11. <https://doi.org/10.17303/jdoh.2022.9.104>
- Hassan, Y. M., Guan, B. H., Chuan, L. K., Hamza, M. F., Khandaker, M. U., Sikiru, S., Adam, A. A., Sani, S. F. A., Abdulkadir, B. A., & Ayub, S. (2022). The influence of ZnO/SiO<sub>2</sub> nanocomposite concentration on rheology, interfacial tension, and wettability for enhanced oil recovery. *Chemical Engineering Research and Design*, 179, 452–461. <https://doi.org/10.1016/j.cherd.2022.01.033>
- Ibraheem, R. (2022). Rheological properties of resin composite. <https://biomatj.com/ojs/index.php/main/article/view/5>
- Kundie, F., Azhari, C. H., Mughtar, A., & Ahmad, Z. A. (2018). Effects of filler size on the mechanical properties of polymer-filled dental composites: A review of recent developments. *J. Phys. Sci*, 29(1), 141–165. <https://doi.org/10.21315/jps2018.29.1.10>
- Majid, M., Hassan, E.-D., Davoud, A., & Saman, M. (2011). A study on the effect of nano-ZnO on rheological and dynamic mechanical properties of polypropylene: experiments and models. *Composites Part B: Engineering*, 42(7), 2038–2046. <https://doi.org/10.1016/j.compositesb.2011.04.043>
- Mandal, S. K., Kumar, R., Rizwee, M., & Kumar, D. (2024). Tuning thermal and structural properties of nano-filled PDMS elastomer. *Polymer Composites*, 45(16), 14832–14844. <https://doi.org/10.1002/pc.28804>
- Papaspyridakos, P., Vazouras, K., Chen, Y. W., Kotina, E., Natto, Z., Kang, K., & Chochlidakis, K. (2020). Digital vs conventional implant impressions: a systematic review and meta-analysis. *Journal of Prosthodontics*, 29(8), 660–678. <https://doi.org/10.1111/jopr.13211>
- Pesce, P., Nicolini, P., Caponio, V. C. A., Zecca, P. A., Canullo, L., Isola, G., ... & Menini, M. (2024). Accuracy of full-arch intraoral scans versus conventional impression: A systematic review with a meta-analysis and a proposal to standardise the analysis of the accuracy. *Journal of Clinical Medicine*, 14(1), 71. <https://doi.org/10.3390/jcm14010071>
- R. Mohd, N., Omar, R. A., & Etajuri, E. A. (2021). Dimensional Stability of Elastomeric Impression Material After Disinfection Via Immersion and Microwave Irradiation. *The Open Dentistry Journal*, 15(1), 658–663. <http://dx.doi.org/10.2174/1874210602115010658>
- Reddy, M. S., Sunaina, D. H., Sharma, S., Jampana, V. R., Namburu, L. S., & Rizwanulla, C. M. R. (2024). Evaluation of Antimicrobial Activity and Physical Properties of Vinyl

- Siloxane Ether Impression Material Modified with Zinc Oxide and Chitosan Nanoparticles: An In-vitro Study. *Journal of Clinical & Diagnostic Research*, 18(7). <https://doi.org/10.7860/JCDR/2024/69938.19664>
22. Savin, C., Antohe, M.-E., Balan, A., Sirghe, A., & Gavrilă, L. (2019). Study regarding the elastic impression biomaterials dimensional stability. *Rev. Chim.(Bucharest)*, 70, 797–800. <https://revistadechimie.ro/pdf/11%20SAVIN%203%2019.pdf>
  23. Utrera-Barrios, S., Yu, L., & Skov, A. L. (2025). Revisiting the Thermal Transitions of Polydimethylsiloxane (PDMS) Elastomers: Addressing Common Misconceptions with Comprehensive Data. *Macromolecular Materials and Engineering*, 2500075. <https://doi.org/10.1002/mame.202500075>
  24. Wang, Y., Cai, Y., Zhang, H., Zhou, J., Zhou, S., Chen, Y., Liang, M., & Zou, H. (2021). Mechanical and thermal degradation behavior of high-performance PDMS elastomer based on epoxy/silicone hybrid network. *Polymer*, 236, 124299. <https://doi.org/10.1016/j.polymer.2021.124299>